Electronic Supplementary Information

2,5-Thiophene Substituted Spiro-bisiloles - Synthesis, Characterization, Electrochemical Properties and Performance in Bulk Heterojunction Solar Cells

Kassem Amro, Anil K. Thakur, Joëlle Rault-Berthelot, Cyril Poriel, Lionel Hirsch, William E. Douglas, Sébastien Clément and Philippe Gerbier

Contents

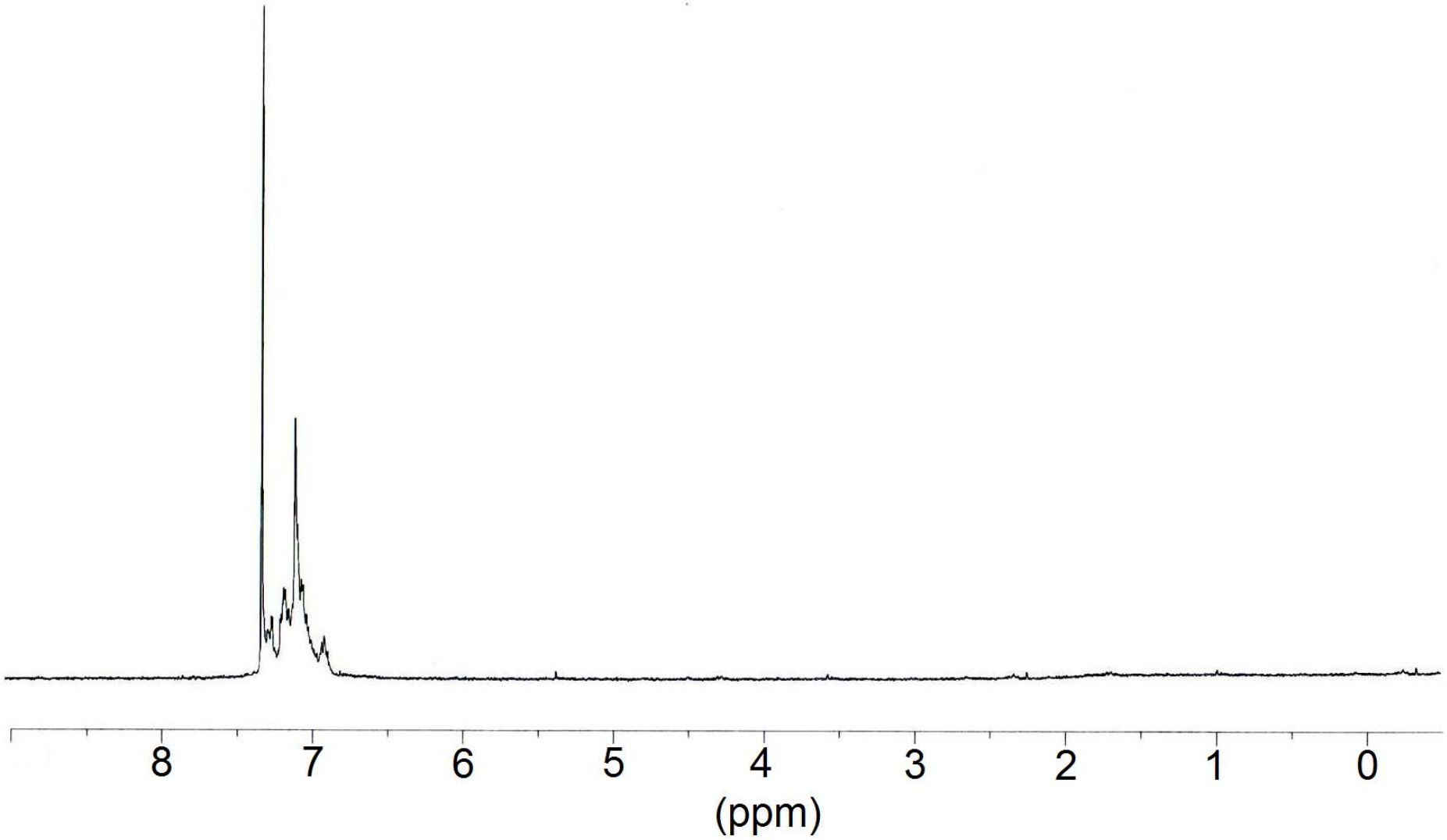

Figure S1. ^{1}H NMR spectrum of **DTSBS** in $CDCl_3$.

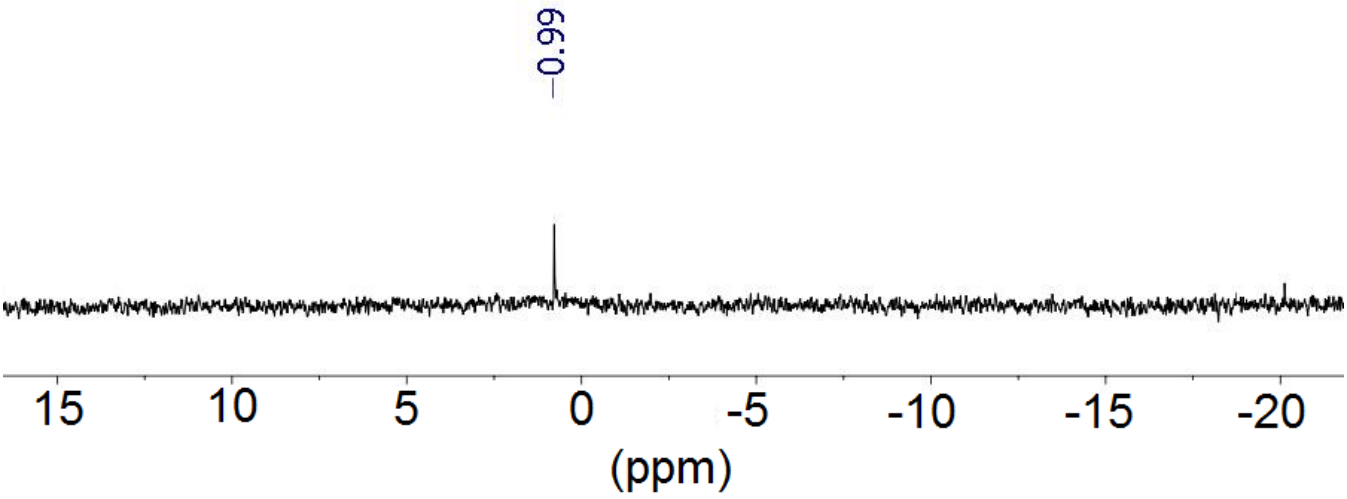

Figure S2. $^{29}Si\{^{1}H\}$ NMR spectrum of **DTSBS** in $CDCl_3$.

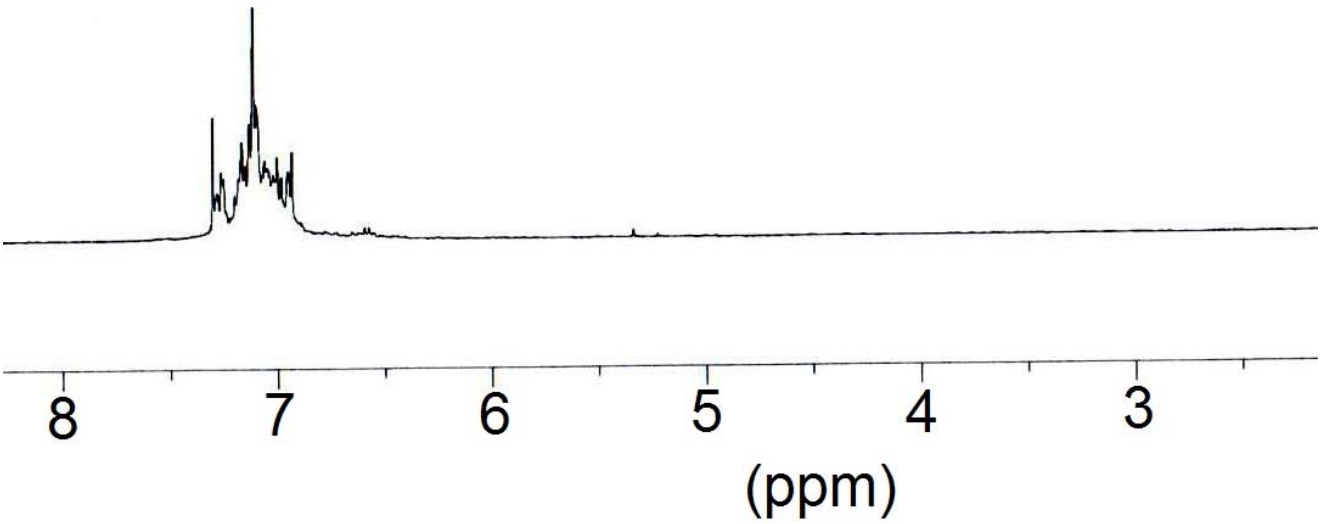

Figure S3. ^{1}H NMR spectrum of **BBTSBS** in $CDCl_3$.

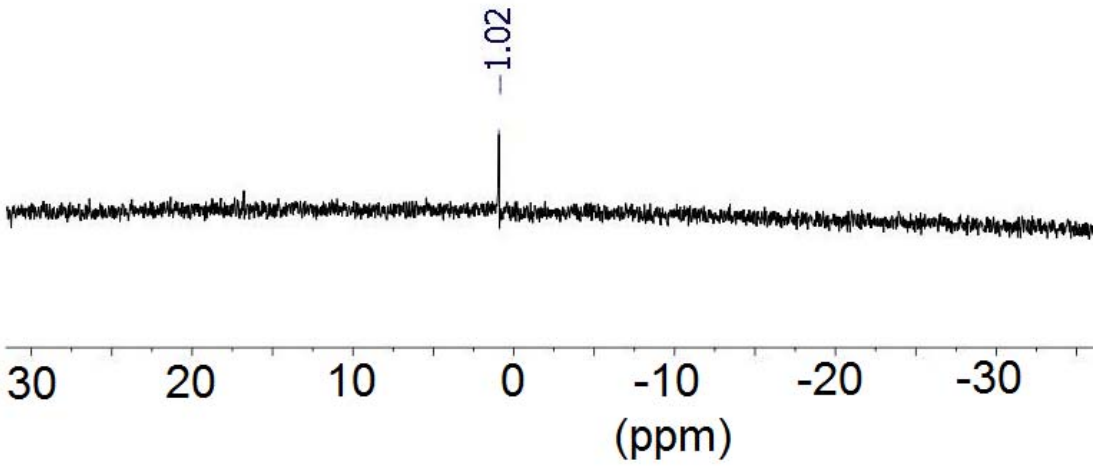

Figure S4. $^{29}Si\{^{1}H\}$ NMR spectrum of **BTSBS** in $CDCl_3$.

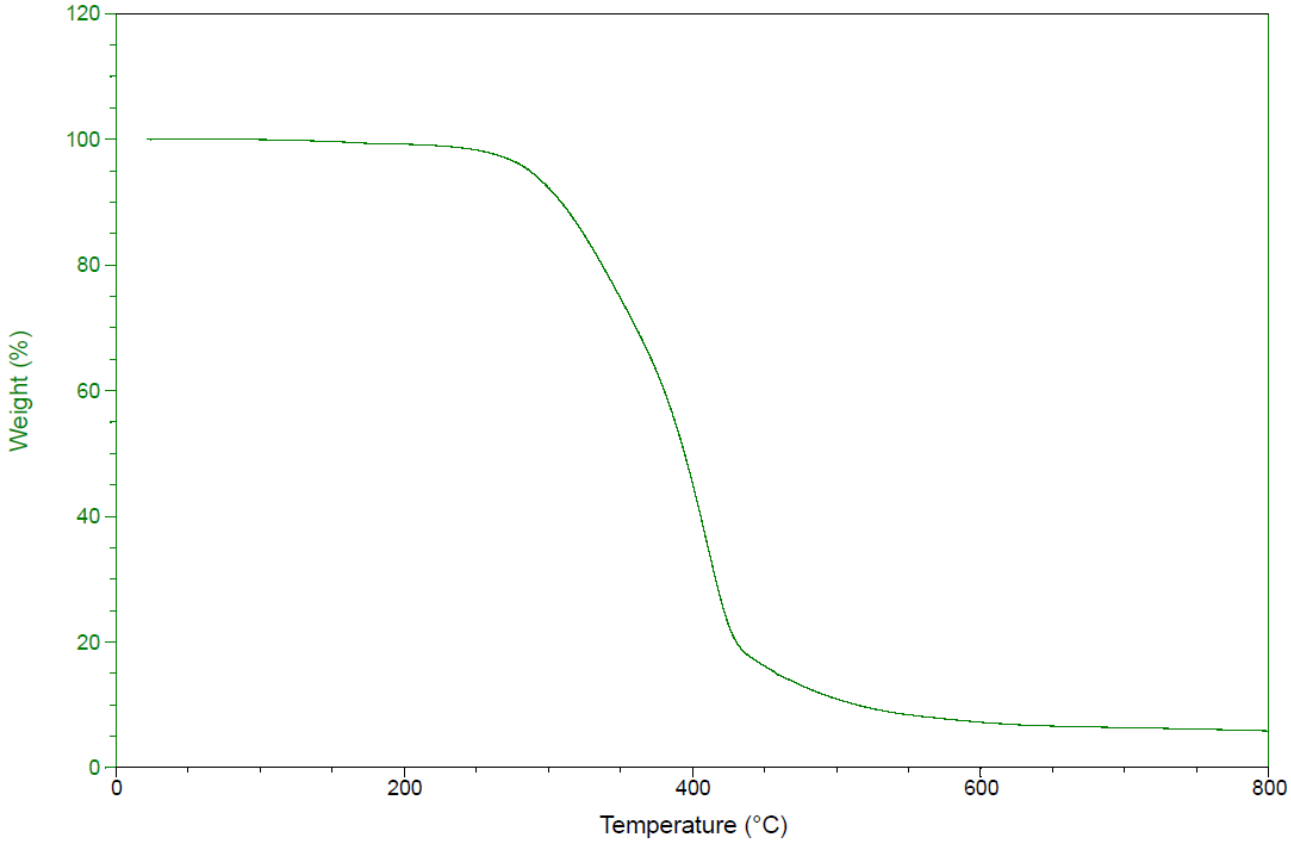

Figure S5. TGA trace for **DTSBS**.

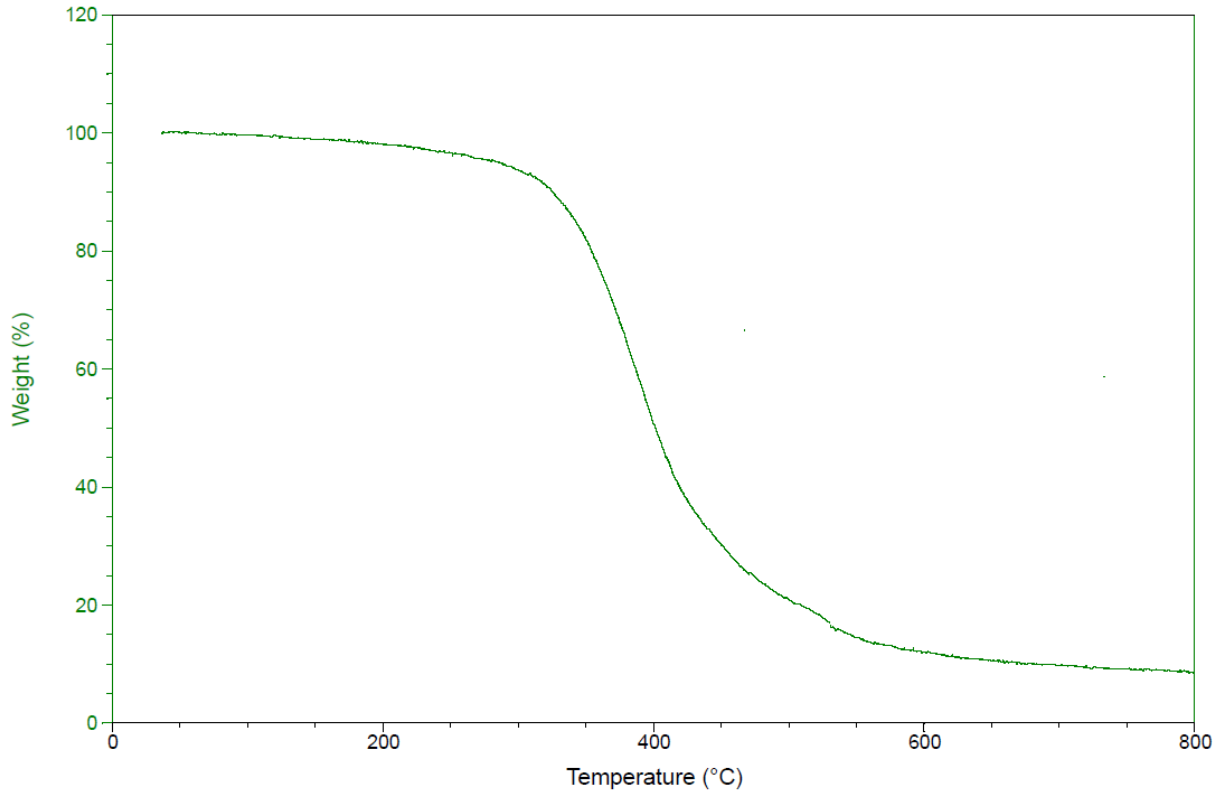

Figure S6. TGA trace for **BBTSBS**.

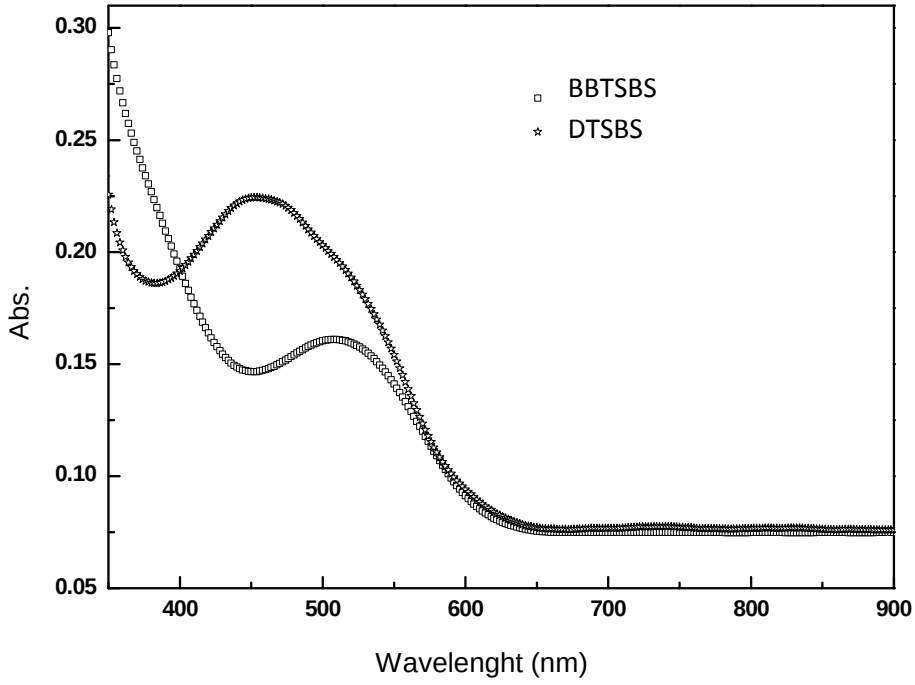

Figure S7. Absorption of **BBTSBS** and **DTSBS** in thin film.

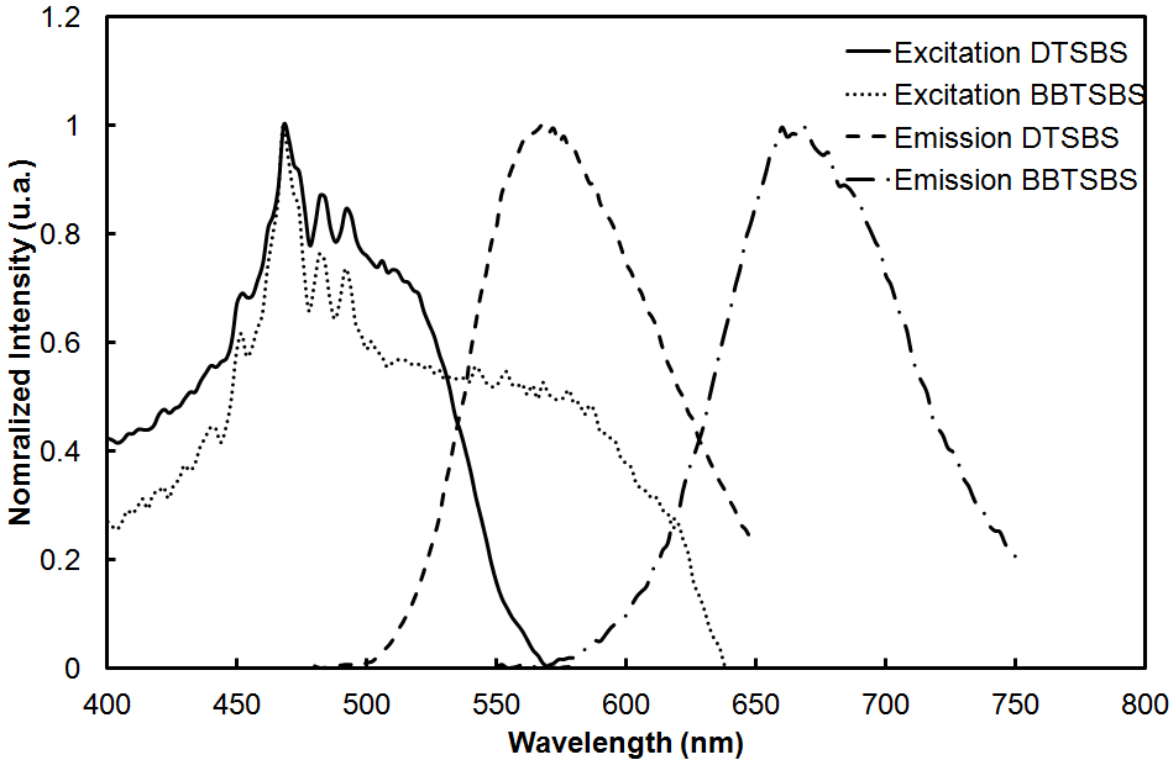

Figure S8. Excitation and emission spectra in the solid state for **DTSBS** and **BBTSBS**.

Calculations :

The geometries were optimized by DFT calculations at the UB3LYP/6-31G level of theory. Energies were calculated at the UB3LYP/6-31G* level of theory. All calculations were carried-out with the Gaussian 03 program package.[1]

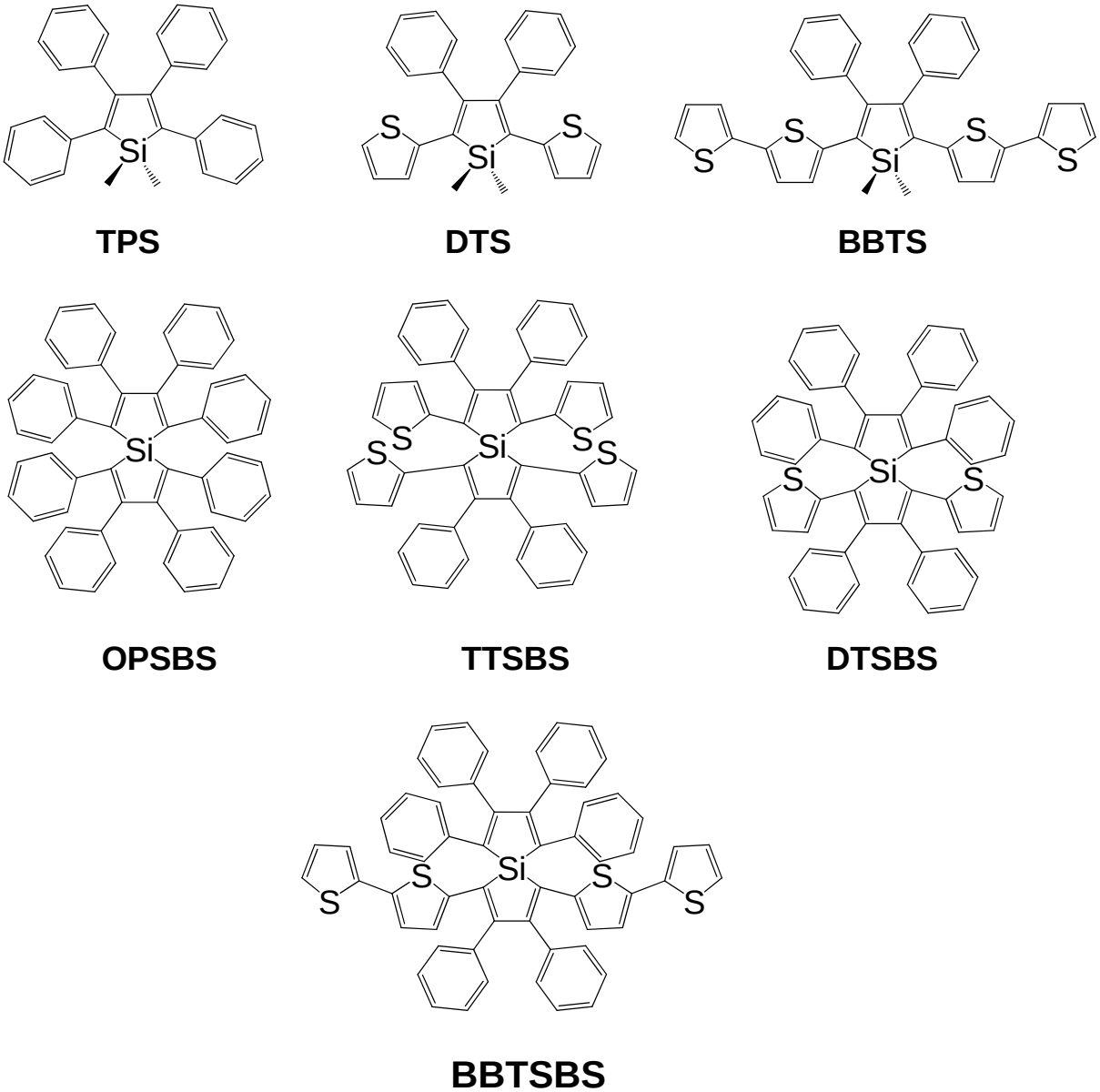

Figure S9. Structure of the siloles and spirosiloles studied herein.

	HOMO-2	HOMO-1	HOMO	LUMO	LUMO+1	LUMO+2
TPS		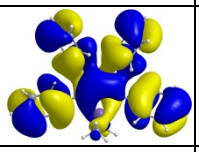	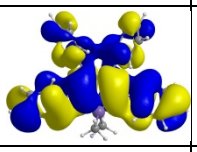	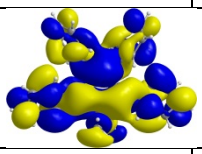	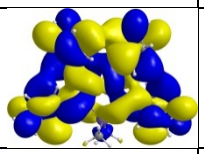	
		-6.33 eV	-5.53 eV	-1.87 eV	-0.64 eV	
DTS		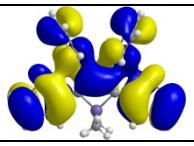	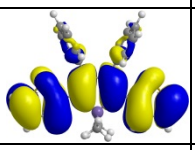	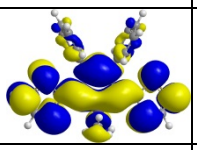	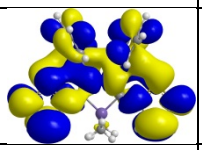	
		-6.47 eV	-5.17 eV	-2.18 eV	-0.78 eV	
BBTS			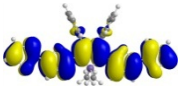	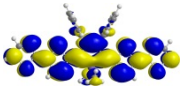	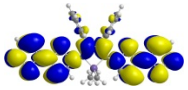	
		-5.84 eV	-4.93 eV	-2.54 eV	-1.65 eV	
OPSBS	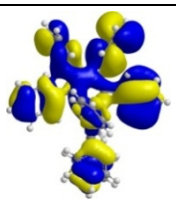	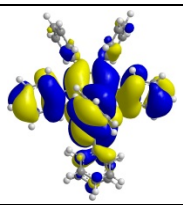	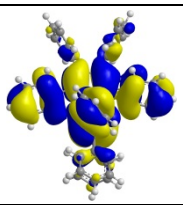	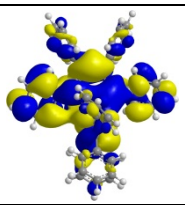	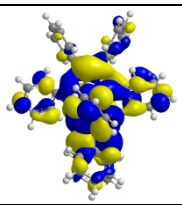	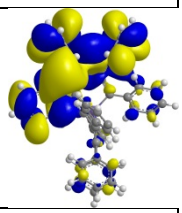
	-6.66 eV	-5.64 eV	-5.49 eV	-2.05 eV	-2.01 eV	-0.61 eV
TTSBS	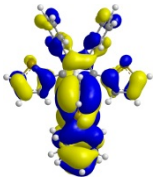	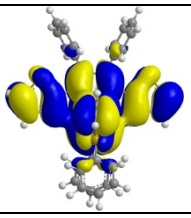	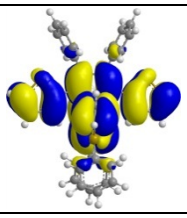	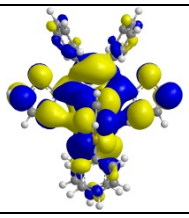	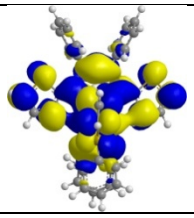	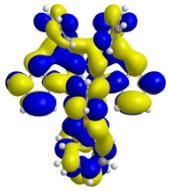
	-6.54 eV	-5.32 eV	-5.22 eV	-2.41 eV	-2.32 eV	-0.87 eV
DTSBS	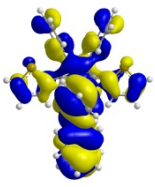	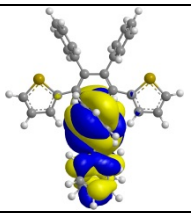	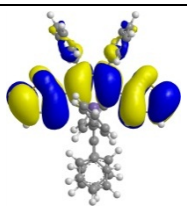	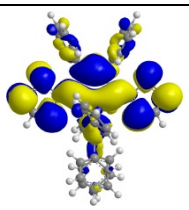	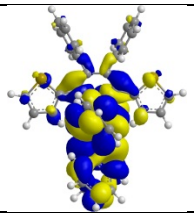	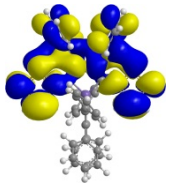
	-6.43 eV	-5.69 eV	-5.21 eV	-2.31 eV	-2.13 eV	-0.82 eV
BBTSBS	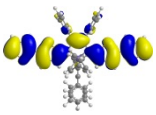	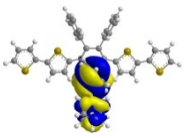	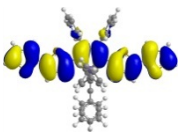	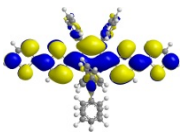	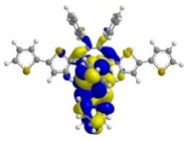	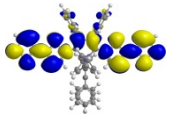
	-5.82 eV	-5.69 eV	-4.94 eV	-2.61 eV	-2.17 eV	-1.65 eV

Figure S10. Kohn-Sham frontier orbitals and corresponding energies of the siloles and spirobisiloles.

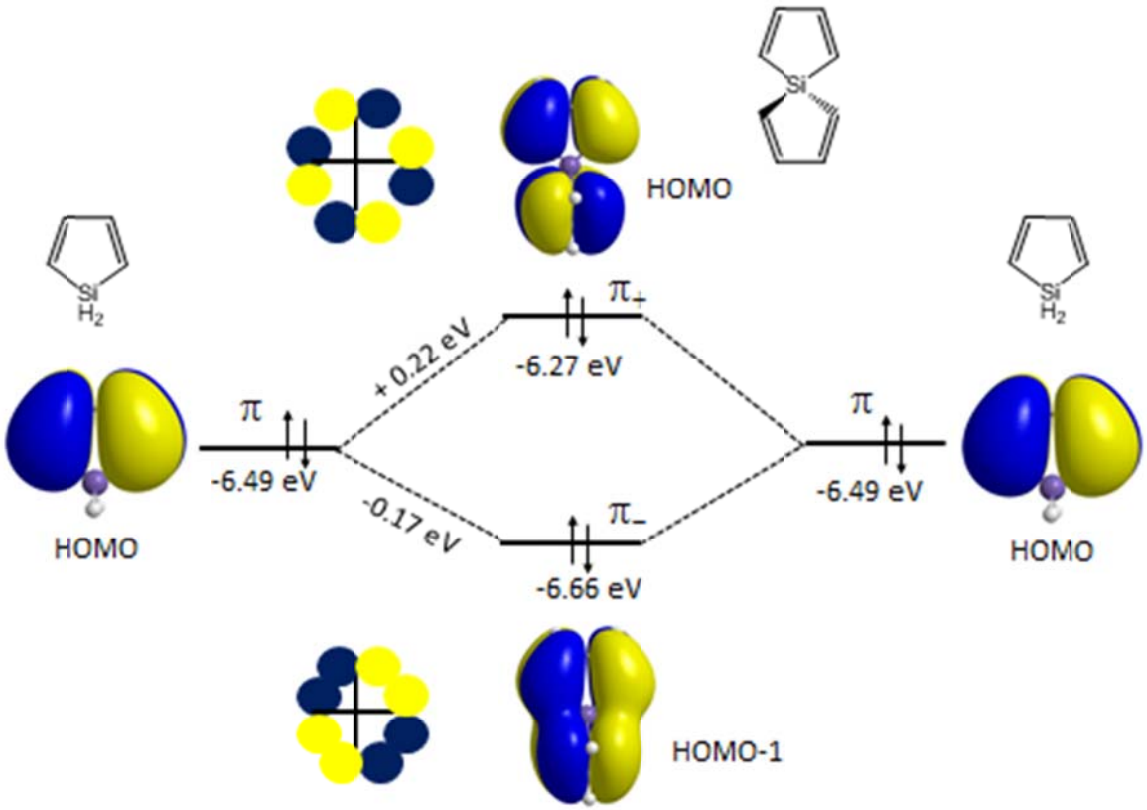

Figure S11. Illustration of the HOMO-HOMO interaction of two spirolinked bisilole rings exhibiting spiroconjugation.

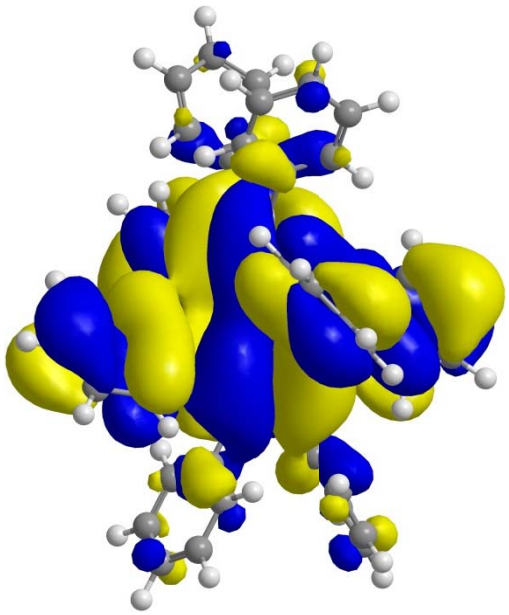

Figure S12. HOMO-1 Kohn-Sham orbital of OPSBS showing the overlap of the two π orbitals on the silole moieties giving rise to spiroconjugation.

	HOMO-1	HOMO
DTSBS	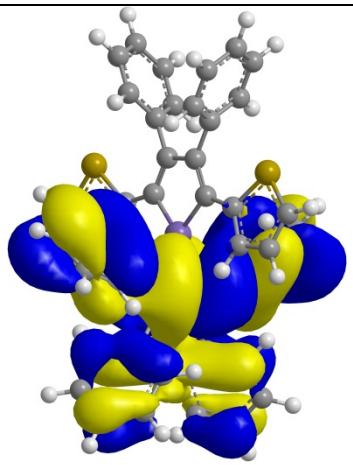	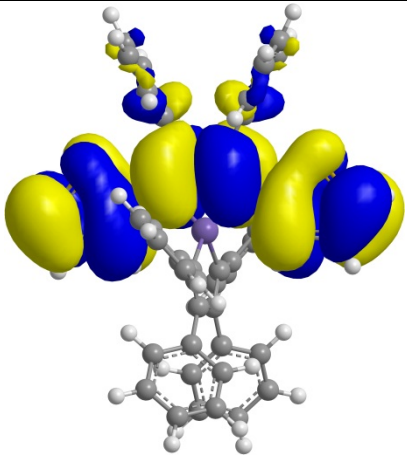
BBTSBS	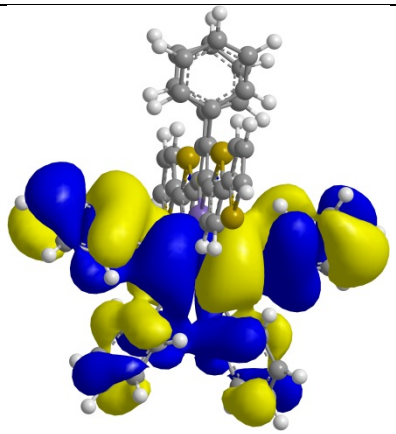	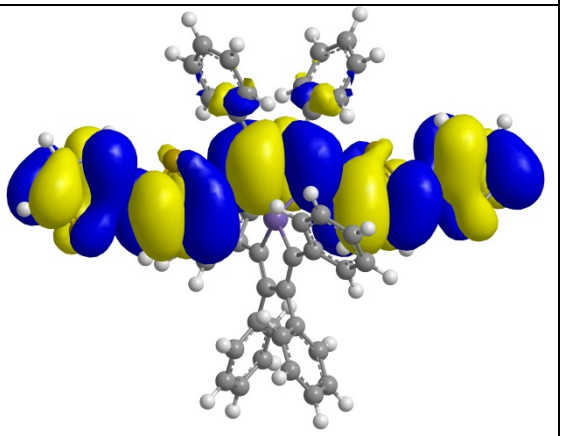

Figure S13. Views of Kohn-Sham HOMO-1 and HOMO of DTSBS and BBTSBS.

	LUMO	LUMO+1
DTSBS	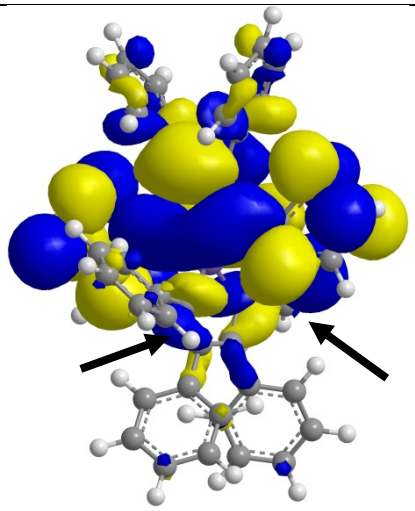	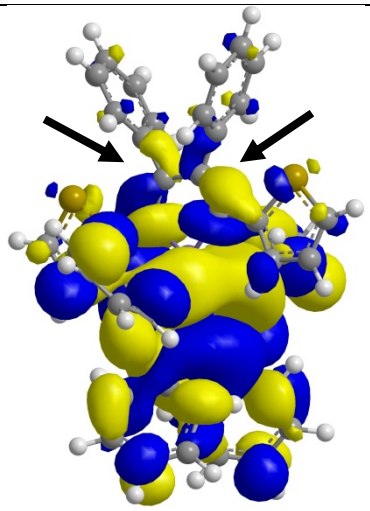
BBTSBS	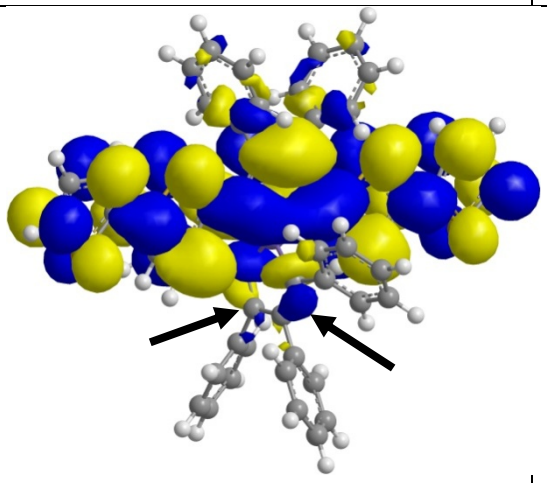	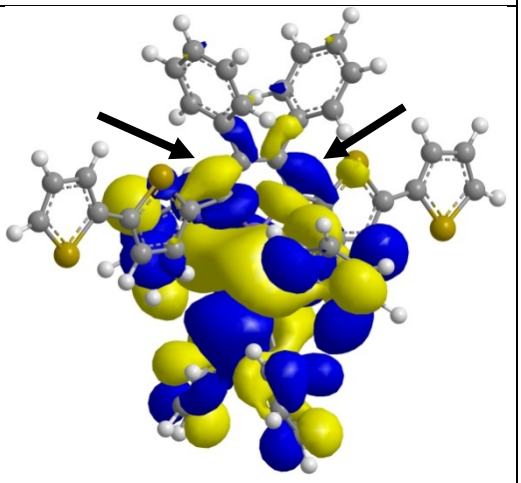

Figure S14. Views of Kohn-Sham LUMO and LUMO+1 of DTSBS and BBTSBS. The arrows indicate the location of the σ* orbitals orbitals involved in the σ*-π* hyperconjugation.

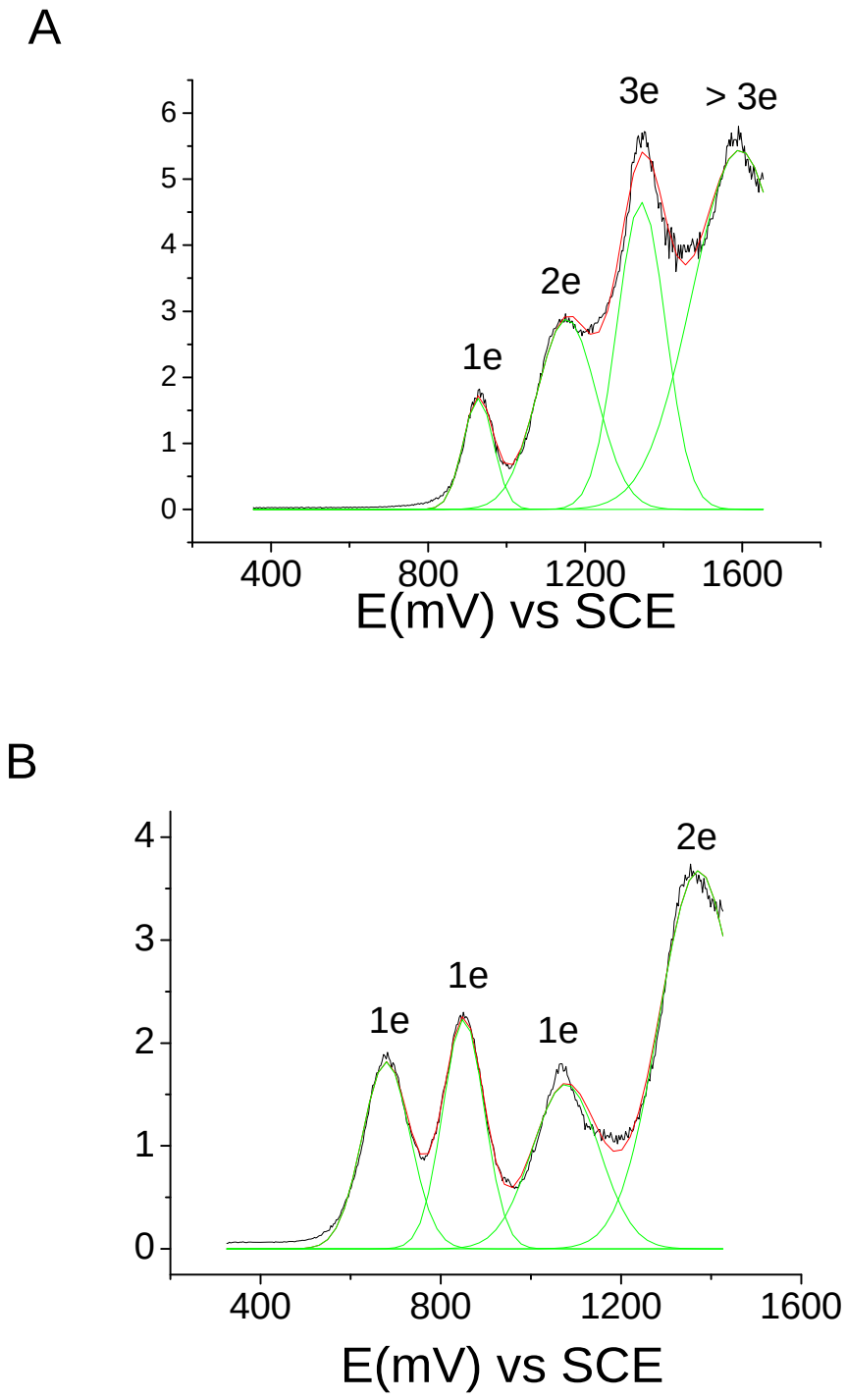

Figure S15. In black : Experimental DPV recorded in CH_2Cl_2-$[NBu_4][PF_6]$ 0.2 M, in the presence of **DTSBS** ($9.8\ 10^{-3}$ M) in A and of **BBTSBS** ($3.2\ 10^{-3}$ M) in B. In red: fit of the experimental data with the sum of four individual Gaussian peaks depicted in green.

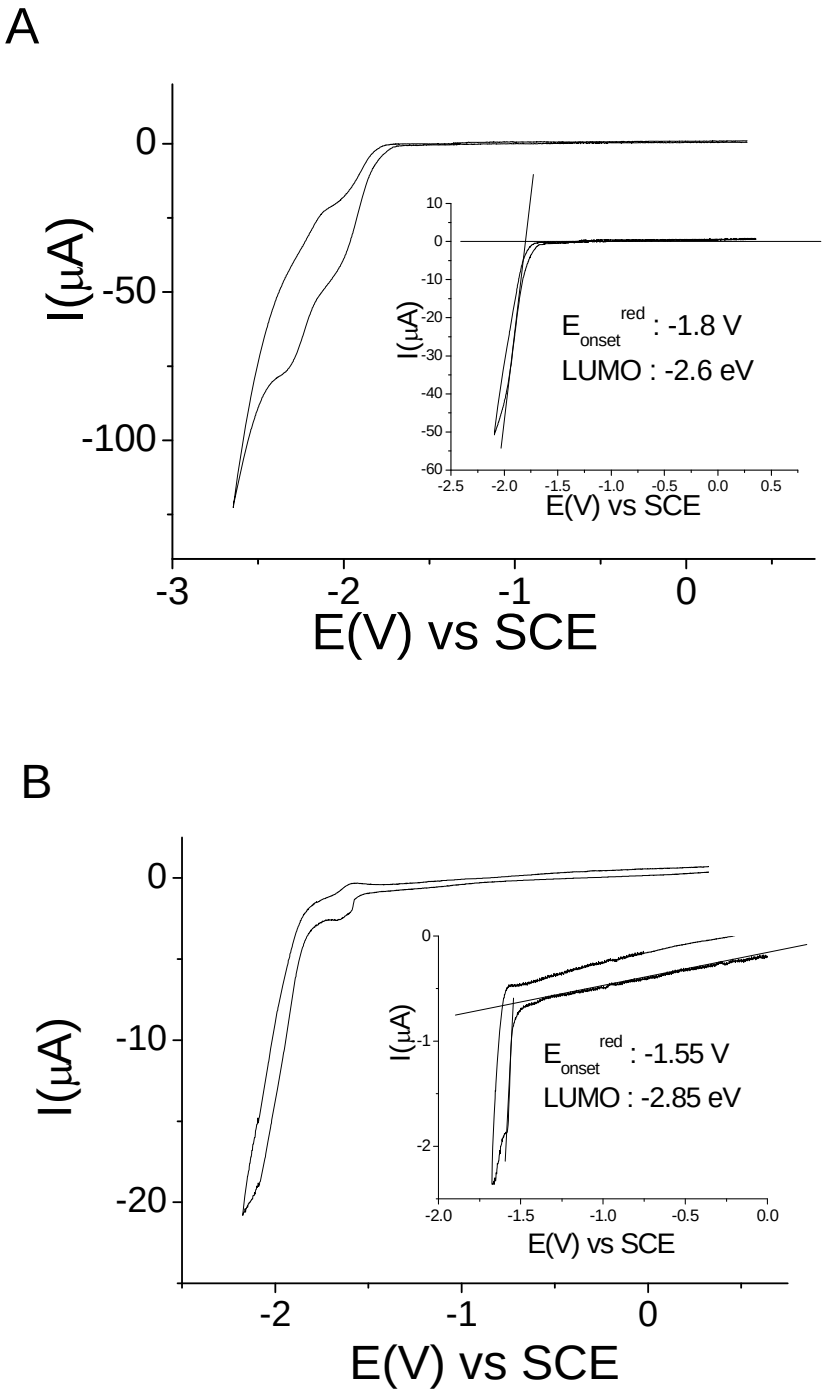

Figure S16. Cyclic voltammetry in CH_2Cl_2-$[NBu_4][PF_6]$ 0.2 M. in the presence of **DTSBS** ($9.8\ 10^{-3}$ M) in A and of **BBTSBS** ($3.2\ 10^{-3}$ M) in B. One cycle between 0.35 and -2.35 V in A and 0.33 and -2.17 V in B. Insets in A and B: zoom on the first reduction wave and E_{onset}^{red} and LUMO determination. Working electrode: 1 mm diameter Pt disk, Sweep-rate : 100 mV/s.

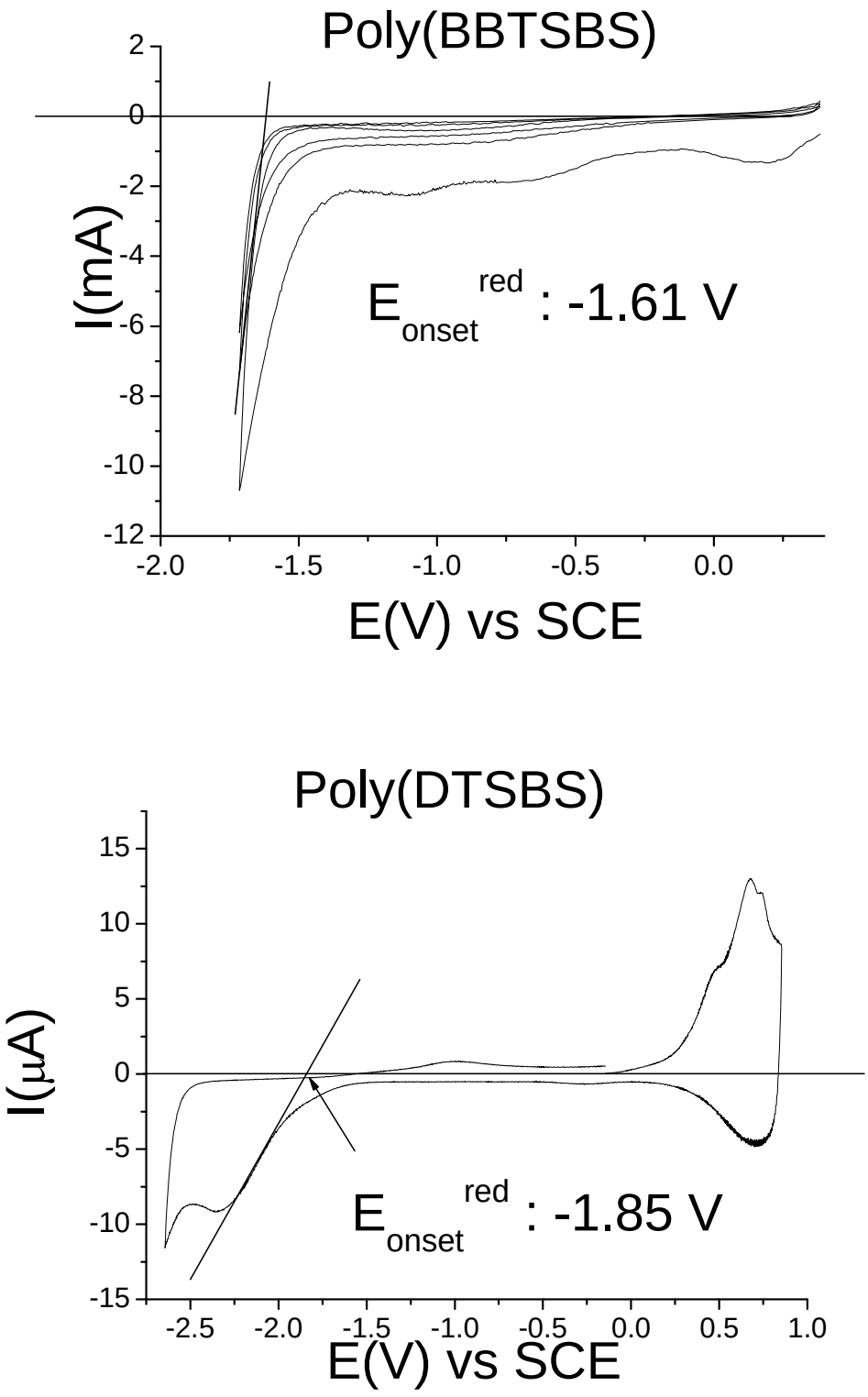

Figure S17. Cyclic voltammetry in CH_2Cl_2-[NBu_4][PF_6] 0.2 M. of a working electrode (1 mm diameter, Pt disk) modified by a deposit of **poly(BBTSBS)** and of **poly(DTSBS)**. Sweep-rate : 100 mV/s.

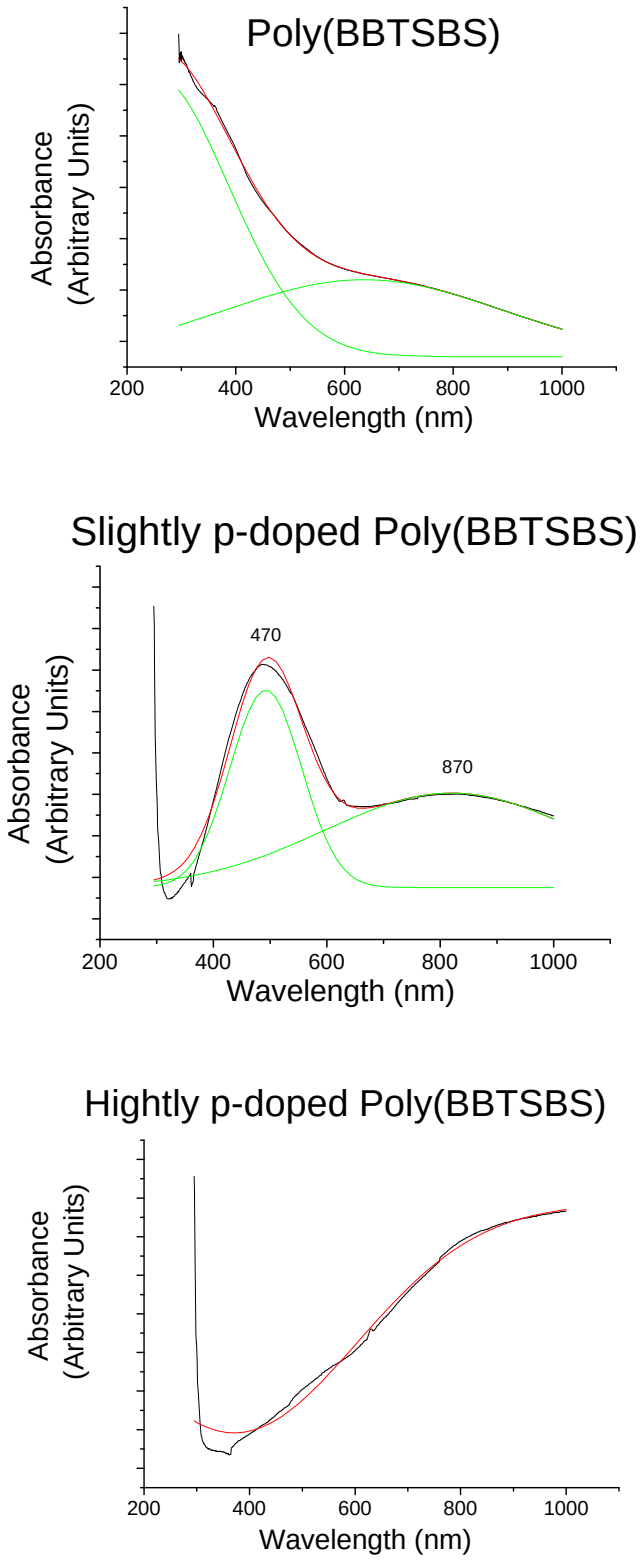

Figure S18. UV visible spectroscopy of neutral, slightly *p*-doped and highly *p*-doped **poly(BBTSBS)** electrogenerated by anodic oxidation of **BBTSBS** on an ITO glass electrode.

References.

1. Gaussian 03, Revision D.02, M. J. Frisch, G. W. Trucks, H. B. Schlegel, G. E. Scuseria, M. A. Robb, J. R. Cheeseman, J. A. Montgomery, Jr., T. Vreven, K. N. Kudin, J. C. Burant, J. M. Millam, S. S. Iyengar, J. Tomasi, V. Barone, B. Mennucci, M. Cossi, G. Scalmani, N. Rega, G. A. Petersson, H. Nakatsuji, M. Hada, M. Ehara, K. Toyota, R. Fukuda, J. Hasegawa, M. Ishida, T. Nakajima, Y. Honda, O. Kitao, H. Nakai, M. Klene, X. Li, J. E. Knox, H. P. Hratchian, J. B. Cross, V. Bakken, C. Adamo, J. Jaramillo, R. Gomperts, R. E. Stratmann, O. Yazyev, A. J. Austin, R. Cammi, C. Pomelli, J. W. Ochterski, P. Y. Ayala, K. Morokuma, G. A. Voth, P. Salvador, J. J. Dannenberg, V. G. Zakrzewski, S. Dapprich, A. D. Daniels, M. C. Strain, O. Farkas, D. K. Malick, A. D. Rabuck, K. Raghavachari, J. B. Foresman, J. V. Ortiz, Q. Cui, A. G. Baboul, S. Clifford, J. Cioslowski, B. B. Stefanov, G. Liu, A. Liashenko, P. Piskorz, I. Komaromi, R. L. Martin, D. J. Fox, T. Keith, M. A. Al-Laham, C. Y. Peng, A. Nanayakkara, M. Challacombe, P. M. W. Gill, B. Johnson, W. Chen, M. W. Wong, C. Gonzalez, J. A. Pople, Gaussian, Inc., Wallingford CT, 2004.